High Resolution Radar Precipitation Evaluation

Dennis A. Miller[1*], Shaorong Wu[1,2], David Kitzmiller[1], and Feng Ding[1,2]

[1]NOAA National Weather Service, Office of Hydrologic Development Silver Spring, MD
[2]Wyle Information Systems LLC, McLean, VA

1. INTRODUCTION

Since the summer of 2008, the Weather Surveillance Radar-1988 Doppler (WSR-88D) has had the capability to process base reflectivity data at eight times higher spatial resolution than previously (250 m x 0.5º vs. 1000 m x 1.0º). While this "super-resolution" is only being applied to some base radar products during the initial phase of implementation, we wish to determine what benefits may be achieved from its application to rainfall accumulation products such as those of the WSR-88D Precipitation Processing System (PPS). For example, higher radar spatial resolution may be expected to result in better detection of small-scale, heavy rain patterns and, in turn, better distribution of that rain to topographic features such as small-scale stream basins. However, these potential benefits might be offset by factors known to cause discrepancies between quantitative precipitation estimates (QPE) determined aloft and the amounts and distribution of rainfall realized at the ground, including sub-beam advection, evaporation, and hydrometeor interactions. Indeed, the impact of these factors may be exacerbated when QPEs are analyzed at finer spatial scales.

The goal of this research is to investigate the potential for realizing improved accuracy in radar-based precipitation estimates – and subsequently, improved results in hydrological applications, such as stream flow and river height forecasts – from the processing of radar reflectivity data at the higher spatial resolutions now available. We will also endeavor to make an initial recommendation as to whether WSR-88D precipitation products should be upgraded to a finer spatial resolution. Focus herein will be on the exploration of this question via performance of gauge-radar statistical evaluations.

Dennis.Miller@noaa.gov, 1325 East West Highway, Silver Spring MD 20910

2. APPROACH

We utilized a methodology analogous to the WSR-88D PPS (Fulton et al. 1998) to generate one-hourly (clock-hourly) radar accumulation estimates, via the traditional "Z-R" relationship, across a span of discrete spatial resolutions ranging from approximately that of the new super resolution ("super res") to approximately that of the legacy WSR-88D. Coarser resolution estimates were determined from the finer resolutions by successively aggregating reflectivity power in the radial direction. We then performed statistical correlation and error analyses upon the radar accumulation sets at each resolution against a matching set of accumulations derived from co-located rain gauges, in closely-spaced networks.

We employed two datasets for the study. The primary dataset, which contributed over 8,500 gauge-radar (G-R) pairs, was from an experimental system deployed in east-central Florida during the summer of 1998 ("TEFLUN"; see Habib and Krajewski 2002). Radar data were from the National Center for Atmospheric Research (NCAR) S-band, dual polarization, Doppler radar known as "S-Pol", and the rain gauge data were collected within NASA's Tropical Rainfall Measurement Mission-Ground Validation (TRMM-GV) network. The finest spatial resolution of the S-Pol data was 0.15 km

x 1.0°, approximately 20% larger than the super-res volume at any range. The S-Pol sample bins were aggregated in multiples of 150 m to yield six levels of analysis: 150m; 300m; 450m; 600m; 750m; and 900m.

Another dataset, containing over 750 qualifying G-R pairs, was created from precipitation estimates from the NOAA/National Severe Storms Laboratory (NSSL) research-prototype WSR-88D radar (KOUN), located in Norman, Oklahoma (Ryzhkov et al. 2005a), and coincident, 1-h rain gauge reports from the Oklahoma Mesonet (McPherson et al. 2007), during the warm seasons of 2004 and 2005. The KOUN sample bins were aggregated in multiples of 250 m to yield four levels of analysis: 250m; 500m; 750m; and 1000m.

For both datasets, QPEs were determined only from the 0.5^0 elevation scan, using the default (i.e. 'Convective') Z-R relationship from NEXRAD:

$$Z = a R^b$$

where Z = backscattered Reflectivity Power (mm^6/m^3); R = Rainfall Rate (mm/hr); a = 300; and b = 1.4. The radar sampling frequency was approximately five minutes, meaning that data from ~13 volume scans were typically used to calculate the one-hour radar accumulation estimates.

Our analysis methodology involved three phases. In Phase 1, which was undertaken for both pairs of datasets, we evaluated all G-R pairs with non-zero gauge or radar hourly accumulation under the entire radar umbrella. For the primary dataset, we also performed statistical analyses for the following situations: after stratification of the G-R pairs into annular rings by distance from the radar; after application of a higher threshold for minimum rainfall amount; and after application of a threshold for rainfall gradient. In the second and third phases, which were performed only on the primary dataset, we focused on densely packed sub-clusters of gauges. These clusters covering areas <20 km^2 and each containing four-to-seven gauges spaced as closely as 1-km, could be considered representative of idealized networks of small basins In Phase 2, we performed statistical analyses on all the individual G-R pairs in each cluster, similarly to as in Phase 1. In Phase 3, we performed the analyses after averaging all the hourly gauge and matching radar values (at each spatial resolution) together within each cluster to produce mean areal precipitation (MAP) estimates.

For each of these configurations at each aggregation level, some or all of the following statistical parameters were determined: Radar Mean Accumulation (after correction for Mean Field Bias); Ratio of (corrected) radar accumulation to gauge accumulation; Correlation Coefficient (r); Mean Absolute Error (MAE); Root Mean Square Error (RMSE); and Standard Deviation of the Absolute Error (SD).

3. RESULTS FROM OTHER STUDIES

Studies of TRMM ground validation data with related goals were reported by Habib and Krajewski (2002) and by Gebremichael and Krajewski (2004), though their primary focus was on spatial variability of rainfall and its relationship to gauge-radar correlations in general.

More recently, Knox and Anagnostou (2009) reported on the effects of interpolating high-resolution QPEs from an X-band radar unit to grids with mesh lengths varying from 300 to 5000 m, regarding grid to point gauge rainfall correlations. They reported that grid mesh length had only rather minor effect on correlation statistics such as rainfall detection and RMS error for accumulation periods from 15 to 60 minutes, though some improvement in scores was evident for finer grid mesh lengths. Potentially important differences between this study and ours are that all radar-gauge correlation estimates were based on rain gauges less than 25 km from the radar, and the scanning frequency was only 1 minute, much less than the 4-6 minutes necessitated by general weather surveillance as carried out by the

WSR-88D. Also, the Knox and Anagnostou study was based on light-moderate rainfall events, while ours contained numerous cases of intense subtropical convection.

4. RAIN GAUGE DATA AND QUALITY CONTROL

For our principal dataset, the distribution of gauges within a radius of 171 km from the S-Pol unit is shown in Fig. 1. The figure shows only the 125 gauges retained after the QC procedures explained below. Because part of our study dealt with the ability of the radar to represent small-scale spatial variability in rainfall, attention was also focused on several sub-networks or 'clusters', highlighted in the figure.

The rain gauge data were quality controlled through several steps. We first eliminated gauge sites with uncertain locations due to conflicts in available metadata. We then compared rainfall time series of closely located gauges against one another and against the trace from the collocated grid box of the (hourly) Digital Precipitation Array (DPA) product from the WSR-88D radar at Melbourne Florida (KMLB). If, by subjective determination, a portion of one gauge's trace differed substantially from that of the other gauge and the DPA product, those reports were eliminated. Finally, if a radar sample bin corresponding to a gauge, at any resolution, showed evidence of clutter contamination, the sample bins at all the aggregations, as well as the gauge, were removed.

5. OVERVIEW OF WEATHER DURING TEST PERIOD (FLORIDA)

The weather situation for our primary dataset during the course of the experiment (20 July to 29 September 1998) was typical of mid-to-late summer over Florida, with some intense local rainfall and some cases with mesoscale organization of precipitation features. Data from 27 days were utilized. Overall, approximately 37% of the hourly gauge reports indicated measurable rainfall ≥ 0.25 mm; 11% had ≥ 2.5 mm, and about 0.7% had ≥ 25 mm.

6. ANALYSIS PHASE 1: ALL G-R PAIRS WITHIN RADAR UMBRELLA CONSIDERED

In this phase, linear correlation and error statistics were calculated based on radar-gauge pairs meeting the criterion that either a gauge or radar value must be non-zero. This was done first for all G-R pairs under the radar umbrella (8687 pairs qualified, in total), then for subsets of those pairs falling within the three discrete range-bands: near: 0-67 km; middle: 67-106km; far: 106-171 km. A conceptual depiction of this phase of the analysis is shown in Fig. 2, and results for the various G-R statistical measures are contained in Table 1. It is seen in the table that, with this minimal, non-zero criterion for G-R pairs there is little discernible difference in results across the radar spatial resolutions, either under the entire radar umbrella or in any of the range bands. Not once is the condition found wherein the difference between the 'best' and 'worst' results for a statistical measure reaches 0.05, implying no appreciable operational significance.

There is a possibility that these results are due to light precipitation and small spatial gradients in the rainfall fields, which predominate even in convective rainfall. We therefore repeated the above statistical procedures for the following, more restrictive situations: 'moderate-heavy' rain; and 'substantial precipitation gradient' (indicative of sharp differences across the spatial analysis range). The criteria for our categories were: 'moderate-heavy': at least one sample bin among the (six) aggregations (150m, 300m, …, 900m) incorporating the rain gauge, or the gauge, itself, has an hourly accumulation >= 10.0 mm (532 of the 8687 total pairs qualified, or 6.1%); and 'substantial gradient': the difference between the 'heaviest' and 'lightest' hourly accumulations among the aggregations is >= 2.5 mm (144 pairs, or 1.7%, qualified). These analyses were again determined for all qualifying G-R pairs under the radar umbrella, and then

stratified into three range bands, as in Table 1. The results for these situations are shown in Tables 2 & 3, respectively.

Analysis of the root-mean squared and mean absolute error statistics reveals that in no situation was the difference between the 'best' result (i.e. smallest mean-absolute error;) and the 'worst' result deemed to be "statistically significant" when assessed at the conventional, 5% likelihood level. This was determined by applying a t-test with a condition of there being less than a 5% probability of an observed difference being due to random variation. However, we felt that, in some situations, minor but consistent trends toward meaningful differences were revealed. In Tables 2-3, if the difference between the 'best' and 'worst' result for a statistical measure across the six resolutions is greater than 5%, the 'best' result is noted in **bold** and the 'worst' result in ***bold italics***.

In Table 2, it is seen that for 'moderate-heavy' rain situations, when the entire radar umbrella is considered (532 G-R pairs, total), a slight tendency emerges for "better" results at the finer resolutions than the coarser (e.g. MAE 7.54 mm at 150 m res. vs. 7.65 mm at 900 m res; RMSE, likewise, 10.77 mm vs. 10.82 mm). When also stratified by range, some more noteworthy differences are observed. At mid ranges (67-106 km), "better" results are seen at the finer than the coarser resolutions for all our statistical measures – by an amount exceeding 5% for the 'MAE' fields and not exceeding 5% for the 'SD' and RMSE' fields. The same tendency, though less pronounced, is observed in the near range band – 0-67 km. At far ranges (106-171 km), though, the opposite tendency emerges – i.e. for all statistical measures, the "best" result occurs at the coarsest resolution (900 m) and the "worst" result at the finest resolution (150 m), with the differences in all instances exceeding our 5% threshold criterion.

In Table 3, containing the results for the 'substantial gradient' situations, (144 G-R pairs, total), the same general situation is observed as was for the 'moderate-heavy' rain cases. That is, under the entire radar umbrella, somewhat "better" results are seen at the finer, rather than the coarser, resolutions. This tendency, here, is observed most strongly in the near range band and, to a lesser extent, at the middle ranges, while a fairly pronounced reversal is, again, observed at far ranges.

We then repeated the above analysis – though only for all non-zero G-R pairs under the entire radar umbrella – for our Oklahoma datasets, for three rain events during the warm seasons of 2004 and 2005. During this period, the dual-polarization WSR-88D prototype operated by NSSL routinely collected reflectivity and other moments at a bin resolution of 250 m and beamwidth of 1º (Ryzhkov et al. 2005a). We prepared 1-h rainfall estimates from the horizontally-polarized, base reflectivity field at the original resolution and aggregated in the radial direction to 500, 750, and 1000 m. While no additional quality control was attempted, this reflectivity data was filtered by an early version of the Hydrometeor Classification Algorithm (Park et al. 2009), which appeared to be effective at reducing returns from biota and ground clutter. Rain gauge reports were from sites within the mesoscale surface network operated by the Oklahoma Climate Survey. The gauge reports indicated some hourly amounts in excess of 25 mm. A bias factor adjustment of 0.477 was applied to the radar estimates to correct a consistent high bias relative to the gauge reports.

As shown in Table 4, statistics compiled for 754 gauge/radar pairs indicate only minor impacts from the differing degrees of spatial averaging. The 1000-m estimates featured the lowest RMS errors and highest correlations relative to the gauge reports, but the statistics from the various sets of estimates differed by only a few per cent. These results, obtained from a dataset geographically well-removed from the Florida TEFLUN testbed and from a different radar, confirmed our earlier findings for the situation when all gauge-radar pairs with precipitation under the radar umbrella were considered.

7. ANALYSIS PHASE 2: GAUGE-RADAR SPATIAL CORRELATION WITHIN SMALL GAUGE NETWORKS

The second phase of the experiment was designed to determine if spatial aggregation of the radar data had an effect on representation of the spatial rainfall pattern, and not necessarily the absolute amount. This question is important because some NWS operational practices are based on the assumption that the radar can properly depict sharp spatial gradients in rainfall and differentiate between rain amounts over adjacent, small basins. Therefore, we examined the spatial correlations between radar and gauge estimates within small sub-networks or clusters of closely-located gauges occupying only a few tens of km^2. A conceptual depiction of this phase of the analysis is shown in Fig. 3.

Six such 'clusters' were identified (refer to Fig. 1). An individual hour's data was included when the difference between the largest and smallest 1-h gauge report was at least 2.5 mm, to insure some appreciable variability in the small-scale rainfall pattern. The gauge and radar estimates for that hour were ranked by order of amount and then correlated. We found that, for most clusters in individual hours, the radar did show appreciable skill in depicting the rainfall distribution over these very small areas. That is, for 1-h rainfall, in many cases the gauge-radar correlation (across all levels of aggregation) within the gauge network was ≥ 0.7 (indicating ~50% reduction of variance).

Shown in Table 5 are the Mean Correlations as a function of aggregation distance over all qualifying hours, and the Fraction of Hours for which the gauge-radar correlation was ≥ 0.7, with the clusters ordered from highest to lowest in terms of overall correlation (i.e. average of the Mean Correlations). For each cluster, the Mean Separation Distance among the gauges and the Mean Range of the gauges from the radar are also shown.

Findings overall were quite similar to those of Phase 1 (when all G-R pairs under the radar umbrella were considered) – i.e. no significant differences among the aggregation distances This result generally held among all six 'clusters', indicating, again, that the spatial aggregation of the radar data had relatively little effect on the correlations to rain gauge reports. It should be noted that the variations in correlation statistics within clusters as a function of aggregation distance were relatively minor compared to other factors concerning the clusters as a whole, such as the distance of their centroids from the radar or the average separation distance among their constituent gauges.

8. ANALYSIS PHASE 3 – GAUGE-RADAR CORRELATION FOR SMALL-AREA MEAN PRECIPITATION

In the final phase of the experiment, gauge and radar values for individual gauge points were each separately aggregated within the network clusters. These values approximate gauge and radar mean-areal precipitation (MAP) such as might be observed over small stream basins. Spatial aggregation might have some effect on radar MAPs because, with greater aggregation, precipitation immediately outside the area would be included. A conceptual depiction of this phase of the analysis is shown in Fig. 4.

Correlation measures between the gauge-based and radar-based areal precipitation were higher than the point values shown in Phase I, as might be expected given the spatial smoothing implied in the areal-averaging procedure. However, as before, the degree of radar spatial aggregation generally was found to have little effect on the gauge-radar MAP correlations or errors.

9. SUMMARY, CONCLUSIONS, AND FUTURE WORK

Examination of the results indicates that, overall, we found relatively small differences, of no operational significance,

in our statistical measures of QPE accuracy across the range of fine-to-coarse spatial resolution, particularly when the entire radar umbrella was considered. We did, though, find some tendency toward better results at the finer resolutions in some situations, including: 1) large precipitation amounts; 2) large precipitation gradients; and 3) at near and mid–range distances from the radar, where (we conjecture) neither low-altitude contamination, such as from residual clutter, AP, radar side lobes or biota, nor sub-beam effects, such as from wind advection, are likely to play a significant role. In no situations, however, did these tendencies reach measures that would be considered "statistically significant", when measured against the standard criterion of there being less than a 5% probability of an observed difference being due to random variation. Therefore, these results may indicate that there could be an advantage in achieving more accurate rainfall estimates when base radar data are available – and analyzed – at finer resolutions, but only in certain circumstances. We would not, at this time, recommend that the PPS products be upgraded to the higher, super resolution in WSR-88D operations.

One potential avenue for future study would be to attempt to factor in sub-beam wind effects on falling hydrometeors by performing statistical correlations of individual rain gauges not just with rainfall estimates from the immediately-corresponding sample bin (in which that gauge is contained), but with surrounding sample bins in all directions and within a prescribed distance. If an offset distance and direction (i.e. vector) could be identified that would yield superior results, that vector could then be analyzed against ambient wind conditions (as recorded by ground or upper-air measuring devices or estimated by model). Ultimately, it may prove possible to incorporate ambient wind conditions in a predictive capacity in relating rainfall estimates determined at high spatial resolution, aloft, to distribution of rainfall at the surface.

Another potential future pursuit would be to perform a similar analysis to the above, but with rainfall estimates derived via a dual polar methodology such as that which is to be implemented within WSR-88D operational radars in future years (Ryzhkov et al, 2005b; Giangrande et al. 2008).

Acknowledgements

We are indebted to Scott Ellis and the NCAR staff for assistance with obtaining and interpreting the S-pol radar data. As noted above, rain gauge reports were obtained from the TRMM SVO office. Oklahoma radar data were provided by NSSL (John Krause and Kevin Scharfenberg), and Oklahoma rain gauge data by the Oklahoma Climatological Survey.

REFERENCES

Fulton, R. A., J. P. Breidenbach, D. J. Seo, D. A. Miller, and T. O'Bannon, 1998: The WSR-88D rainfall algorithm. *Weather and Forecasting*, **13**, 377-395.

Gebremichael, M., and W.F. Krajewski, 2004: Assessment of the statistical characterization of small-scale rainfall variability from radar: analysis of TRMM ground validation datasets. *J. Appl. Meteor.*, **43**, 1180–1199.

Giangrande, S.E., and A.V. Ryzhkov, 2008: Estimation of Rainfall Based on the Results of Polarimetric Echo Classification. *J. Appl. Meteor. Climatol.*, **47**, 2445–2462.

Habib, E., and W.F. Krajewski, 2002: Uncertainty analysis of the TRMM ground-validation radar-rainfall products: application to the TEFLUN-B field campaign. *J. Appl. Meteor.*, **41**, 558–572.

HyangSuk Park, A. V. Ryzhkov, D. S. Zrnić, and Kyung-Eak Kim, 2009: The Hydrometeor Classification Algorithm for the Polarimetric WSR-88D: Description and Application to an MCS. *Weather and Forecasting*, **24**, 730–748

Knox, R., and E. Anagnostou, 2009: Scale interactions in radar rainfall estimation uncertainty. *Journal of Hydrologic Engineering*, **14**, 944-953.

McPherson, R.A., and Coauthors 2007: Statewide monitoring of the mesoscale environment: A technical update on the Oklahoma Mesonet. *J. Atmos. Oceanic Technol.*, **24**, 301–321.

Ryzhkov, A.V., T.J. Schuur, D.W. Burgess, P.L. Heinselman, S.E. Giangrande, and D.S. Zrnic, 2005a: The Joint Polarization Experiment: Polarimetric Rainfall measurements and hydrometeor classification. *Bull. Amer. Meteor. Soc.*, **86**, 809–824.

Ryzhkov, A., Giangrande, S., and Schuur, T., 2005b: Rainfall estimation with a polarimetric prototype of WSR-88D. *J of Appl. Meteor.*, **44**, 502-515.

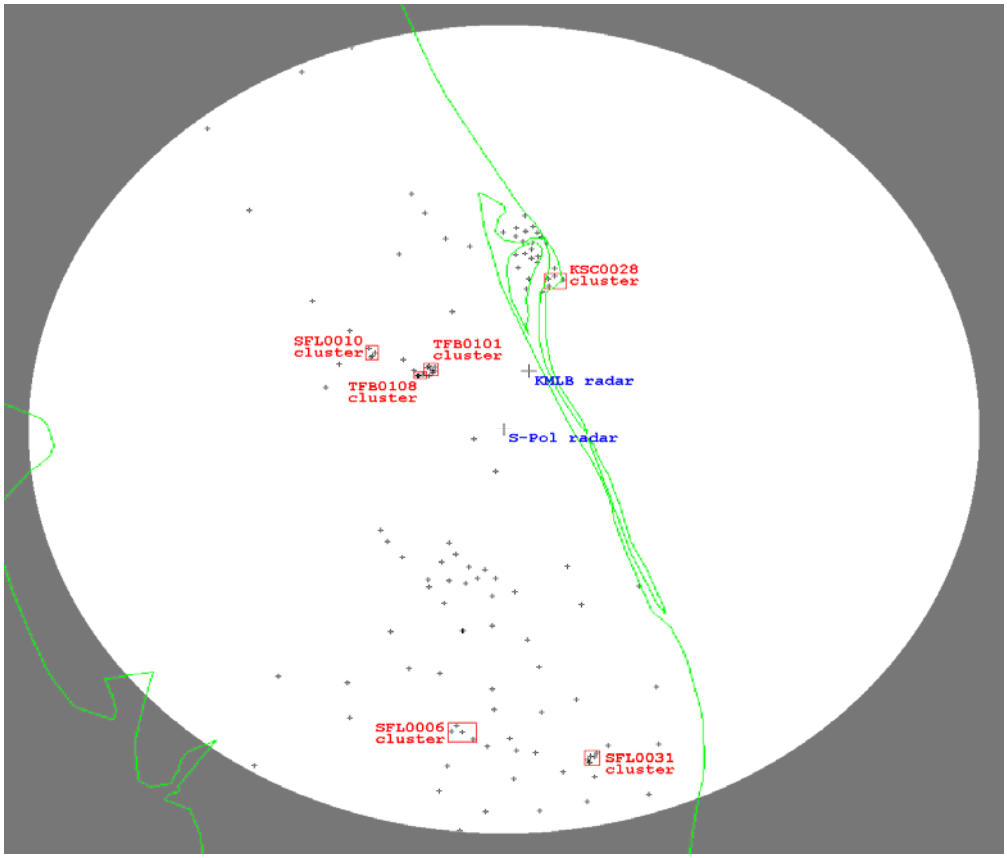

Figure 1. Distribution of gauge sites (small crosses) relative to S-pol radar site (large cross at center). Six sub-networks or 'clusters' of closely-located gauges are shown in red. The white circle indicates a radius of 171 km. WSR-88D Melbourne radar (KMLB) also shown.

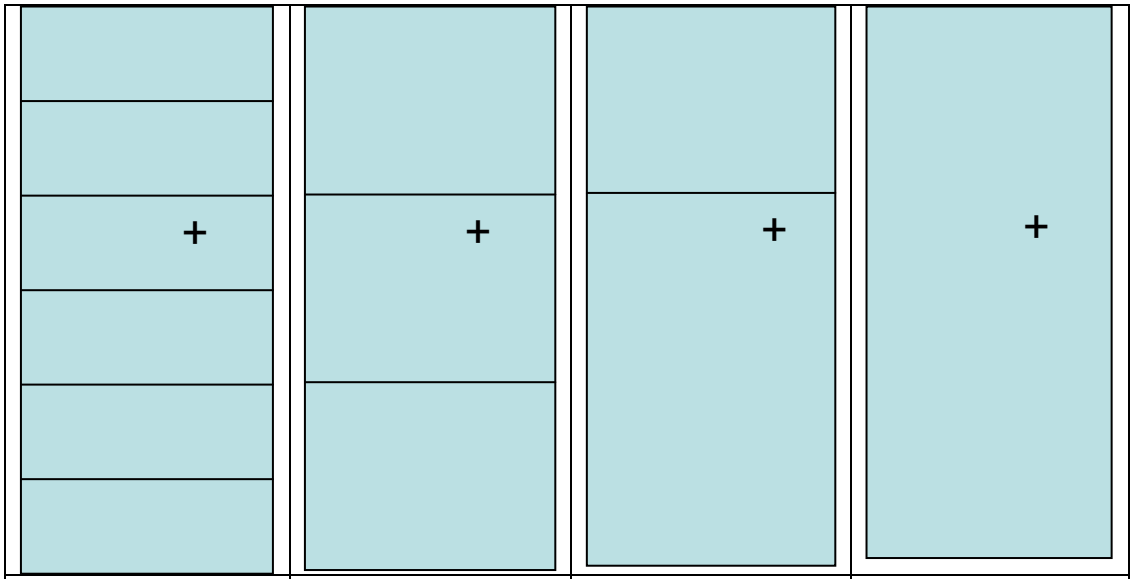

Figure 2. Schematic diagram for radar QPE aggregation in radial direction, Phase 1 (+ indicates rain gauge location). Note that aggregation volumes are not necessarily symmetric about the gauge point – the location of the grid volumes is arbitrary, as is the case in operations.

Table 1. Gauge-radar correlation coefficients, mean absolute errors, standard deviations, and root-mean-squared errors, listed by spatial aggregation distance (resolution) of the radar sample bins. All G-R pairs considered together (1a); then stratified by range (1b-1d). Gauge or radar value is non-zero. (NOTE: No differences across aggregations determined to be "statistically significant", based on t-test applied against standard criterion of a 5% or less likelihood of a difference being due to random variation, for a finding of significance.)

1a. all ranges:	8687 R/G-data-pairs; Gauge mean: 1.81 mm					
Radar	**mean(mm)**	**R/G ratio**	**r**	**MAE(mm)**	**SD(mm)**	**RMSE(mm)**
150m-res	1.78	0.98	0.81	1.07	2.96	2.96
.	.	.	.	.	.	.
900m-res	1.84	1.01	0.81	1.08	2.96	2.96

1b. range 0-67 km:	3360 R/G-data-pairs; Gauge mean: 1.59 mm					
150m-res	1.63	1.02	0.81	0.93	2.85	2.85
.	.	.	.	.	.	.
900m-res	1.70	1.07	0.80	0.96	2.88	2.88

1c. range 67-106 km:	2892 R/G-data-pairs; Gauge mean: 1.82 mm					
150m-res	1.70	0.93	0.85	0.98	2.98	2.98
.	.	.	.	.	.	.
900m-res	1.75	0.96	0.84	1.00	2.99	2.99

1d. range 106-171 km:	2435 R/G-data-pairs; Gauge mean: 2.12 mm					
150m-res	2.10	0.99	0.78	1.35	3.10	3.09
.	.	.	.	.	.	.
900m-res	2.13	1.00	0.79	1.33	3.02	3.02

Table 2. Gauge-radar statistical measures (as in Table 1), with gauge or radar ≥ 10.0 mm. (Note: No differences across aggregations found to be "statistically significant", as explained in Table 1. If absolute difference between 'best' and 'worst' result for any statistical measure is greater than 5%, the 'best' result is noted in **bold** and the 'worst' result in ***bold italics***)

2a. all ranges:	532 R/G-data-pairs; Gauge mean: 17.57 mm					
Radar	**mean(mm)**	**R/G ratio**	**r**	**MAE(mm)**	**SD(mm)**	**RMSE(mm)**
150m-res	17.42	0.99	0.43	7.54	10.78	10.77
300m-res	17.51	1.00	0.44	7.50	10.77	10.76
.	.	.	.	.	.	.
900m-res	17.69	1.01	0.43	7.65	10.83	10.82

2b. range 0-67 km:	178 R/G-data-pairs; Gauge mean: 17.47 mm					
150m-res	18.70	1.07	0.40	8.24	11.90	11.93
300m-res	18.91	1.08	0.40	8.32	11.94	12.00
.	.	.	.	.	.	.
900m-res	19.09	1.09	0.39	8.51	12.10	12.17

2c. range 67-106 km:	172 R/G-data-pairs; Gauge mean: 18.94 mm					
150m-res	17.66	0.93	**0.58**	6.80	10.13	10.18
300m-res	17.72	0.94	**0.58**	**6.72**	10.13	10.17
.	.	.	.	.	.	.
900m-res	18.08	0.95	***0.55***	***7.24***	10.48	10.48

2d. range 106-171 km:	182 R/G-data-pairs; Gauge mean: 16.38 mm					
150m-res	15.94	0.97	***0.24***	***7.55***	***10.12***	***10.10***
300m-res	15.93	0.97	0.25	7.43	10.03	10.01
.	.	.	.	.	.	.
900m-res	15.94	0.97	**0.29**	**7.21**	**9.68**	**9.66**

Table 3. Gauge-radar statistical measures (as in Table 1), with gradient among radar values ≥ 2.5 mm. (Note: No differences across aggregations determined "statistically significant". Notations for 'best' and 'worst' results as in Table 2).

3a. all ranges: 144 R/G-data-pairs; Gauge mean: 12.02 mm

Radar	mean(mm)	R/G ratio	r	MAE(mm)	SD(mm)	RMSE(mm)
150m-res	11.42	0.95	0.81	**6.11**	8.29	8.28
300m-res	11.77	0.98	0.82	6.18	8.21	8.19
.	.	.	.	.	.	.
900m-res	12.40	1.03	0.80	***6.68***	8.53	8.51

3b. range 0-67km 73 R/G-data-pairs; Gauge mean: 10.67 mm

Radar						
150m-res	10.74	1.01	**0.81**	**5.26**	**7.19**	**7.14**
300m-res	11.16	1.05	0.78	5.78	7.51	7.48
.	.	.	.	.	.	.
900m-res	11.77	1.10	***0.74***	***6.42***	***8.14***	***8.16***

3c. range 67-106km 45 R/G-data-pairs; Gauge mean: 14.53 mm

Radar						
150m-res	11.93	0.82	0.90	7.09	9.43	9.68
300m-res	12.23	0.84	0.92	**6.73**	**8.99**	**9.18**
.	.	.	.	.	.	.
750m-res	12.95	0.89	0.88	***7.64***	***9.88***	***9.89***
900m-res	13.47	0.93	0.89	7.47	9.64	9.59

3d. range 106-171km 26 R/G-data-pairs; Gauge mean: 11.49 mm

Radar						
150m-res	12.46	1.08	***0.64***	***6.78***	***8.74***	***8.62***
300m-res	12.66	1.10	0.68	6.36	8.34	8.26
.	.	.	.	.	.	.
900m-res	12.31	1.07	**0.75**	**6.01**	**7.54**	**7.44**

Table 4. As in Table 1, except statistics for 754 gauge/radar pairs over Oklahoma collected during storm events in 2004 and 2005. Gauge or radar value is non-zero. (Note: No differences across aggregations determined "statistically significant". Notations for 'best' and 'worst' results as in Table 2).

4a. all ranges: 754 R/G-data-pairs; Gauge mean: 1.81 mm

Radar	mean(mm)	R/G ratio	r	MAE(mm)	SD(mm)	RMSE(mm)
250m-res	3.36	1.00	0.80	1.77	3.20	3.66
500m-res	3.37	1.00	0.80	1.75	3.18	3.63
750m-res	3.39	1.01	0.81	1.76	3.15	3.61
1000m-res	3.39	1.01	0.81	1.75	3.11	3.57

Table 5. Mean value of gauge-radar linear correlation coefficients within individual rain gauge clusters (subnetworks), averaged over multiple 1-h events, and number of hours in which the gauge-radar correlation was ≥ 0.7. Highest and lowest values of any given field across the range of spatial aggregation are indicated as in Tables 1-4 (in cases of "ties", all are so indicated). The clusters are shown in order of highest to lowest Mean Correlation (averaged over all aggregation distances). (Note: No differences across aggregations determined "statistically significant". Notations for 'best' and 'worst' results as in Table 2).

Cluster KSC0028 (15 hours)

Gauges: 3 or 4; Mean separation 2.99 km; Mean range from radar 65.9 km

Aggreg. dist. (m)	**150**	**300**	**450**	**600**	**750**	**900**	**[Avg]**
Mean Correlation	0.73	***0.67***	0.71	0.72	0.77	**0.78**	[0.73]
Fraction ≥ 0.7	0.67	***0.60***	0.67	0.73	**0.80**	**0.80**	

Cluster SFL0010 (11 hours)

Gauges: 4; Mean separation 1.47 km; Mean range from radar 57.6 km

	150	**300**	**450**	**600**	**750**	**900**	**[Avg]**
Mean Correlation	***0.58***	0.69	0.67	0.63	**0.70**	0.60	[0.64]
Fraction ≥ 0.7	0.73	0.73	***0.64***	**0.82**	**0.82**	***0.64***	

Cluster TFB0101 (14 hours)

Gauges: 5 to 7; Mean separation 0.99 km; Mean range from radar 36.8 km

	150	**300**	**450**	**600**	**750**	**900**	**[Avg]**
Mean Correlation	***0.60***	0.62	0.62	**0.66**	0.62	**0.66**	[0.63]
Fraction ≥ 0.7	***0.64***	***0.64***	***0.64***	**0.79**	0.71	0.71	

Cluster SFL0031 (19 hours)

Gauges: 6; Mean separation 1.04 km; Mean range from radar 143.2 km

	150	**300**	**450**	**600**	**750**	**900**	**[Avg]**
Mean Correlation	0.49	***0.48***	0.49	0.49	**0.55**	***0.48***	[0.50]
Fraction ≥ 0.7	0.47	***0.42***	0.47	**0.53**	***0.42***	**0.53**	

Cluster SFL0006 (18 hours)

Gauges: 4; Mean separation 3.53 km; Mean range from radar 129.4 km

	150	**300**	**450**	**600**	**750**	**900**	**[Avg]**
Mean Correlation	**0.50**	***0.43***	0.47	0.47	**0.50**	0.48	[0.48]
Fraction ≥ 0.7	**0.67**	***0.61***	***0.61***	**0.67**	**0.67**	**0.67**	

Cluster TFB0108 (14 hours)

Gauges: 4; Mean separation 0.76 km; Mean range from radar 38.1 km

	150	**300**	**450**	**600**	**750**	**900**	**[Avg]**
Mean Correlation	0.13	0.23	***0.07***	**0.30**	0.18	**0.30**	[0.20]
Fraction ≥ 0.7	***0.14***	***0.14***	***0.14***	**0.50**	0.21	**0.50**	

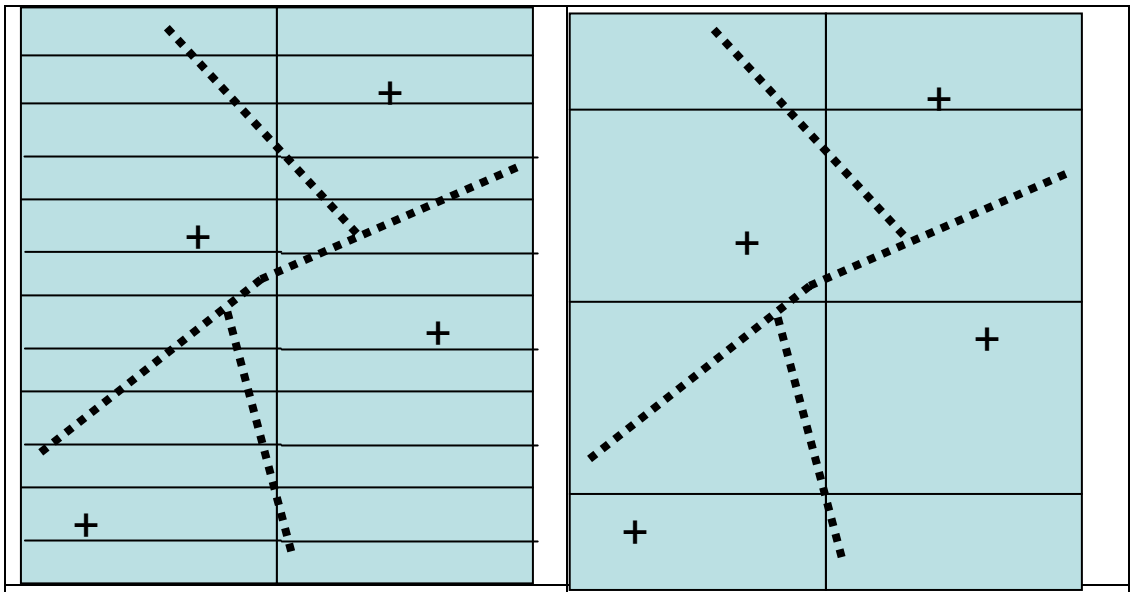

150 meter bins	900 meter bins

Figure 3. Schematic diagram for radar QPE aggregation - patterns, Phase 2. (+ indicates rain gauge locations). Dashed lines indicate basin boundaries. Note: radar sample bins correlating with rain gauges change with radar spatial resolution.

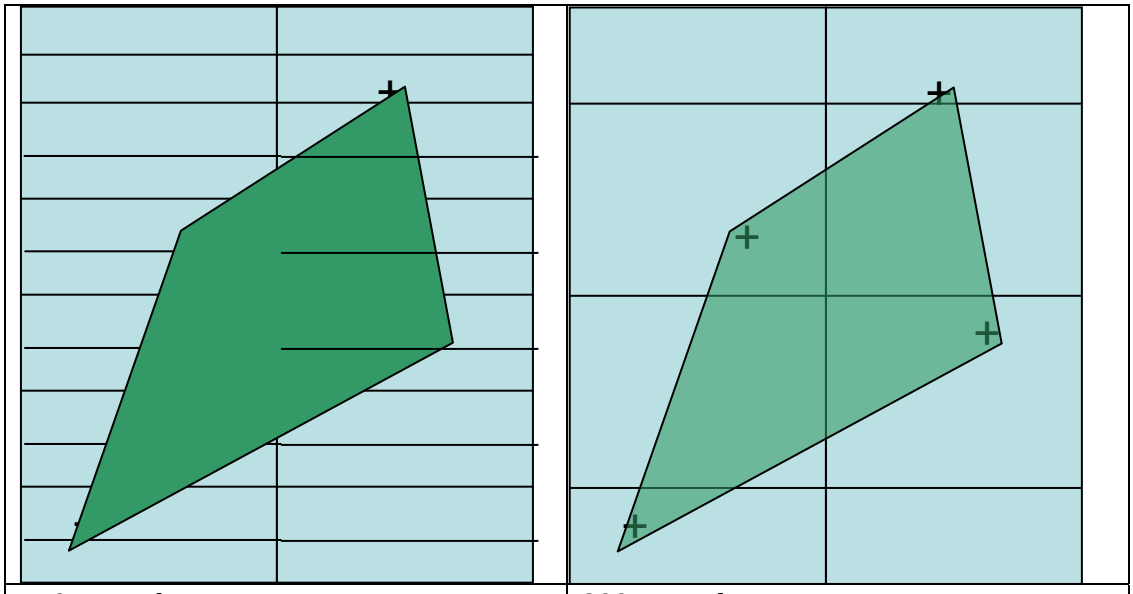

150 meter bins Approximation to Mean Areal Precip is from 4 radar data points.	900 meter bins Approximation to Mean Areal Precip is from 4 different, larger radar data points.

Figure 4. Schematic diagram for radar QPE aggregation – Mean Areal Precipitation (MAP), Phase 3. (+ indicates rain gauge locations). Shaded area represents a basin over which gauges are averaged for MAP.